




## Comparative Review of Gamma Ray Shielding Properties of Building and Metallic Materials Using Experimental and Theoretical Methods

Mohamed Eltayeb Mohamed Eisa 

Department of Physics, College of Science, Northern Border University, Arar 91431, Saudi Arabia

Corresponding Author Email: [memeisa@yahoo.com](mailto:memeisa@yahoo.com)

Copyright: ©2025 The author. This article is published by IIETA and is licensed under the CC BY 4.0 license (<http://creativecommons.org/licenses/by/4.0/>).

<https://doi.org/10.18280/acsm.490306>

### ABSTRACT

**Received:** 2 May 2025

**Revised:** 15 June 2025

**Accepted:** 20 June 2025

**Available online:** 30 June 2025

#### Keywords:

*half-value layer, radiation protection applications, theoretical investigations, superior attenuation properties, notable aspects*

The assessment in this review paper is founded on the synthesis of experimental and theoretical investigations, which methodically appraise the gamma-ray shielding capabilities of prevalent materials. These materials encompass lead (Pb), iron (Fe), concrete, cement, and clay. The evaluation of shielding performance involved the use of gamma sources Cs-137 and Co-60, along with critical metrics such as the half-value layer (HVL) and the linear attenuation coefficient (LAC). The findings demonstrate that lead exhibits superior attenuation properties compared to iron, while clay, cement, and concrete demonstrate significantly inferior attenuating capabilities. The use of composite shielding combinations, such as Pb + Fe and Pb + cement, has been demonstrated to enhance attenuation efficiency. The review underscores two notable aspects. Firstly, it highlights the pressing need for substance optimization in radiation protection applications, and secondly, it outlines the prospective benefits of composite shielding.

## 1. INTRODUCTION

Gamma rays, a highly energetic form of electromagnetic radiation, interact with matter primarily through three fundamental mechanisms: photoelectric absorption this process dominates at low gamma energies (<100 keV), Compton scattering at intermediate energies (100 keV to several MeV), and pair production when photon energies exceed 1.022 MeV. The dominance of each mechanism depends on the energy of the incident gamma photons and the atomic number (Z) of the shielding material. Gamma radiation shielding is of critical importance for ensuring safety in a variety of fields, including nuclear reactor operations, medical diagnostics [1-4], radiotherapy, and industrial radiography. In the context of nuclear power plants [5, 6], the implementation of shielding measures is paramount to prevent the escape of harmful radiation into the environment, thereby safeguarding the well-being of workers and neighboring populations. In the medical context, shielding [7-10] is mandatory in diagnostic imaging and therapeutic applications to restrict patient and staff exposure to ionizing radiation [11]. The International Atomic Energy Agency (IAEA) has historically underscored the significance of effective shielding as a component of its guidelines for radiation protection and nuclear safety standards. As indicated by the extant literature, industrial radiography and radiological facilities [12] also pose substantial risks due to the use of high-energy gamma sources, such as cobalt-60 and cesium-137 [13]. Gamma rays are a form of electromagnetic radiation that possesses a high degree of penetration, and their capacity to ionize atoms renders them particularly hazardous to living tissues and electronic systems. Therefore, effective attenuation of the aforementioned rays

necessitates the utilization of materials characterized by elevated density and high atomic number (Z). The enhancement of photon absorption is facilitated through mechanisms including photoelectric absorption, Compton scattering, and pair production [14, 15]. The selection of an appropriate shielding material is influenced by several practical factors [16]. The evaluation of these parameters encompasses material attenuation performance, as measured by the linear attenuation coefficient (LAC) [17, 18] and the half-value layer (HVL). Additional factors include manufacturing cost, mechanical strength, availability, fabrication ease, and environmental safety. Lead (Pb) [19-22], with an atomic number of 82 and a density of 11.34 g/cm<sup>3</sup>, has been the material of choice for gamma shielding for decades due to its superior attenuation characteristic. A substantial body of research has corroborated its pervasive efficacy in industrial and medical contexts. Nevertheless, despite its apparent advantages, lead is associated with several disadvantages.

The substance under consideration has been demonstrated to be substantial in weight and financially exorbitant. It has also been found to be a significant source of toxicity, thereby constituting a potential hazard to human health and the environment in both its application and subsequent disposal [23]. Consequently, there has been an increased focus on the exploration of alternative shielding materials. Iron (Fe), concrete, cement, and clay [24, 25] are among the most frequently studied alternatives, particularly in architectural and civil engineering applications [26], where structural and radiation protection requirements frequently coincide. The use of these materials is advantageous in two respects: first, they have been demonstrated to be more accessible; secondly, and

this point is of particular relevance to the present discussion, they are also less environmentally damaging than alternative materials. It has been demonstrated, however, that on a per thickness basis these materials are generally less efficient than lead. Nevertheless, due to their extensive accessibility and comparatively reduced expense, they are considered practical solutions for large-scale shielding applications. The present study undertakes a critical evaluation of the gamma-ray shielding effectiveness of various common materials [27, 28], including metals and building composites. This study draws on both theoretical calculations and experimental findings to compare shielding performance, with a particular focus on LAC and HVL values [29-33]. Moreover, it investigates the prospective benefits of hybrid and composite shielding materials [34-38], including lead-iron alloys and layered cement-lead composites. These materials are designed to amalgamate the strengths of their constituents while compensating for the deficiencies of each individual material. Such novel approaches have the potential to provide customized shielding solutions, enhancing protection [39, 40], cost-effectiveness, and sustainability.

This review focuses on evaluating and comparing the gamma ray shielding effectiveness of both conventional and alternative construction materials, with special emphasis on their linear attenuation coefficient (LAC) and half-value layer (HVL) properties. The study aims to bridge the gap between theoretical modeling and practical application by analyzing both experimental measurements and composite material performance [19, 21].

The Objectives of this study to assess shielding capabilities of commonly available materials including: Lead (Pb)Iron (Fe), concrete, cement and clay. Quantify and compare each material's: linear attenuation coefficient (LAC), half-value layer (HVL) and density. Evaluate composite materials, such as Pb+Fe and Pb+Cement, to determine whether combining materials improves attenuation, potential trade-offs in cost, weight, and usability. Investigate the energy dependence of attenuation performance across a range of gamma ray energies (notably at 662 keV and beyond). Determine the applicability of materials in real-world scenarios: Medical imaging rooms, nuclear reactor shielding, Radiation labs, Industrial radiography [24, 26].

However the Scope of this review focuses exclusively on gamma radiation (high-energy photons), excluding neutron or alpha/beta particle shielding. Incorporates both experimental data (e.g., air kerma rate measurements from SSDL Sudan) and theoretical calculations using exponential attenuation laws. Considers pure materials and composites in slab or cubic geometries typically used in structural applications. Emphasizes civil, medical, and nuclear infrastructure, where cost-effective and scalable shielding solutions are essential. This review is intended to support researchers, engineers, and health physicists in selecting or designing shielding materials that balance effectiveness, cost, and safety, while also identifying gaps for future innovation, particularly in the area of composite and lead-free shielding technologies [29, 30, 33].

## 2. METHODOLOGY

Concrete mix, cement mortar, and clay samples were prepared and used independently as shielding materials. The British mix design method was followed to produce concrete with a strength target of 25 N/mm<sup>2</sup>. Cubes of concrete [41]

were cast in two standard sizes: 150×150×150 mm and 100×100×100 mm. Cement mortar was prepared in a ratio of 1:4:0.5 (cement:sand:water) and cast similarly. For clay, an optimum moisture content of 40% was established via a Proctor compaction test. Densities of the shielding materials were as follows: lead (11.34 g/cm<sup>3</sup>), iron (7.87 g/cm<sup>3</sup>), concrete (2.374 g/cm<sup>3</sup>), cement (2.139 g/cm<sup>3</sup>), and clay (1.335 g/cm<sup>3</sup>) [42]. Lead and iron samples were prepared in slab forms of different thicknesses. Measurements were carried out at the Secondary Standard Dosimetry Laboratory (SSDL) in Sudan. Air [43, 44] kerma rate was determined at a reference distance from OB-85 irradiator using gamma sources Cs-137 (662 keV) and Co-60 [45] (1173 and 1332 keV).

Shielding samples were placed at the irradiator exit window. The setup included a UNIDOS Electrometer, ionization chamber, barometer, and thermometer. The dosimetry system calibration was traced to the Physikalisch-Technische Bundesanstalt (PTB) via the IAEA laboratory. The chamber was located 2 meters from the gamma source. Air kerma, defined as the kinetic energy released per unit mass of air, was used to evaluate gamma intensity both with and without shielding samples [46]. Linear attenuation coefficients were derived from the slope of attenuation plots using the exponential attenuation law. Half-value layers were calculated from LAC data to indicate shielding thicknesses required to reduce the radiation intensity by 50%.

### 2.1 Data analysis and attenuation calculations

Gamma rays are eliminated from the beam if they come into contact with the shielding material. The attenuation coefficient, which calculates the shielding material's efficacy, is the total of all interaction probabilities. Therefore, before any material is utilized as a shield, the shielding parameters must be precisely determined [47, 48]. The linear attenuation coefficient (LAC) and the half-value layer (HVL) are two fundamental parameters used to quantify the shielding effectiveness of materials against gamma radiation. These parameters are essential for designing radiation protection systems in nuclear medicine, radiography, industry, and research.

The Lambert-Beer law equation controls the shielding material's ability to reduce radiation intensity (1).

$$I = I_0 e^{-\mu x} \quad (1)$$

where,  $I_0$  refers to the count rate with no shielding material, and  $I$  is the count rate with shielding material of thickness  $x$  and attenuation coefficient  $\mu$ . Taking the natural logarithm on both sides, we obtain Eq. (2).

$$\frac{\mu}{\rho} = \frac{1}{\rho x} \ln \frac{I_0}{I} \quad (2)$$

Using this formula [19, 20], the attenuation coefficient is calculated by measuring the gamma-ray intensity both with and without a shield and with varying thicknesses of shielding material positioned between the source and the detector. Since the mass attenuation coefficient ( $\mu_m$ ) is independent of the material's physical state, it is typically used to compare the shielding properties of various materials. The updated formula for calculation. Design parameters for radiation shielding include mean free path, tenth layer value (TVL), half layer value (HLV), and others [17, 49-51]. HVL is known to be the

width of a material needed to cut the air kerma of an X-ray or gamma ray in HLV Eq. (3).

$$\text{HVL} = \frac{\ln 2}{\mu} \quad (3)$$

Composite materials are engineered by combining two or more constituents with significantly different physical or chemical properties, aiming to enhance performance compared to the individual components. In gamma ray shielding, composites are designed to optimize attenuation efficiency, weight, cost, and environmental safety.

However, mechanistically, composite shielding works by strategically combining high-Z absorbers with low-Z structural binders, enhancing gamma ray attenuation over a wide energy range. This approach leverages different interaction mechanisms photoelectric absorption, Compton scattering, and pair production to create a multifunctional barrier that balances effectiveness with cost, manufacturability, and safety. Future work involves nano-composites, hybrid geometries, and functionally graded materials for optimized, application-specific shielding solutions. High-Z constituent (e.g., Pb): Dominates via photoelectric absorption, especially for low-energy photons. Cement matrix: Adds mechanical stability, lowers weight, and engages in Compton scattering at mid-energy ranges. This result in moderate attenuation with improved formability and reduced toxicity.

Metallic Reinforcement Composites (e.g., Pb + Fe), Iron (Fe) adds structural integrity and magnetic shielding. Enhances secondary electron absorption due to dense electron cloud from both metals. Effective for intermediate to high-energy photons due to enhanced scattering and partial pair production at higher energies. Low-Z Matrix + High-Z Additive (e.g., Clay + Pb), Clay, a low-density, porous material, offers poor shielding on its own. But when combined with fine lead particles or oxides: Scattering pathways increase, enhancing photon interaction probability. Localized Z contrast in the matrix increases probability of photoelectric interaction. And this results in marginal improvement, suitable for low-cost, large-volume applications.

Attenuation coefficient superposition principle

In heterogeneous materials, the effective linear attenuation coefficient  $\mu_{\text{eff}}$  is approximated by Eq. (4):

$$\mu_{\text{eff}} = \sum_i w_i \mu_i \quad (4)$$

where,

$\mu_i$  is the attenuation coefficient of the i-th component.

$w_i$  is the mass or volume fraction.

This principle is nonlinear at higher energies due to secondary photon buildup and scatter effects, but it serves as a first-order model in most cases. The experimental results were tabulated and visualized using graphs to compare shielding efficiency. Composite shielding configurations were also evaluated to determine performance improvements over individual materials. From the standpoint of application, these results facilitate the selection of appropriate materials according to radiation type, requisite protection levels, cost, and environmental factors [52]. The findings indicate that a more sophisticated strategy for radiation shielding is warranted. This strategy involves the use of multi-material combinations that are suited to specific use situations. Finally, the findings suggest the existence of promising avenues for future research. One such avenue pertains to the development of innovative and eco-friendly composite materials that can

perform at least comparably to lead while concurrently diminishing their harmful effects. From an applied perspective, these findings enable the selection of suitable materials based on radiation type, requisite protection levels, cost, and environmental factors. The findings support the implementation of a more sophisticated strategy for radiation shielding, with multi-material combinations being particularly effective in specific application scenarios. In summary, the findings indicate the necessity for further research. This encompasses the development of innovative, eco-friendly composite materials that can demonstrate comparable or superior performance to that of lead while concurrently addressing its detrimental effects.

## 2.2 Energy dependence of attenuation

A collimated gamma-ray source (Cs-137 or Co-60), a detector (like an ionization chamber), and slabs of the test material of varying thicknesses Gamma ray attenuation is highly energy-dependent both LAC and HVL are critical in assessing and comparing radiation shielding materials. While LAC provides a direct measure of gamma attenuation per unit thickness, HVL translates this into a practical shielding design value. These parameters are determined through experimental attenuation measurements or derived theoretically from known material properties and gamma energies, forming the backbone of radiation safety engineering. As the photon energy increases, the probability of interaction with matter decreases, resulting in lower LAC and higher HVL values across all tested materials. For instance, iron's HVL increased from 1.199 cm at 662 keV to 2.065 cm at 2 MeV, a nearly 70% increase, indicating reduced effectiveness at higher energies. This trend is typical due to the shift from photoelectric dominance at lower energies to Compton scattering and pair production at higher energies [53, 54]. Lead, although the most effective at low to moderate energies, also shows reduced performance at higher photon energies, necessitating thicker layers to maintain the same shielding level.

This dependency underscores the need to tailor shielding material selection and thickness to the specific energy spectrum of the gamma radiation source in use.

## 3. RESULTS AND DISCUSSIONS

Table 1 compares the shielding effectiveness of five materials lead, iron, concrete, cement, and clay based on their density, linear attenuation coefficient (LAC), and half-value layer (HVL). Lead (Pb) stands out as the most efficient shielding material with the highest LAC ( $1.121 \text{ cm}^{-1}$ ) and the lowest HVL (0.617 cm), attributed to its high atomic number and density ( $11.34 \text{ g/cm}^3$ ). Iron (Fe) provides a good balance of attenuation and cost [43, 44], with a moderate LAC of  $0.463 \text{ cm}^{-1}$  and HVL of 1.496 cm. Concrete and cement, common in structural shielding, show reduced effectiveness, with LACs of  $0.151$  and  $0.139 \text{ cm}^{-1}$ , and HVLs of 4.593 and 4.965 cm, respectively. Clay, despite being naturally abundant, performs poorly as a shield due to its low density ( $1.34 \text{ g/cm}^3$ ) and the highest HVL of 6.779 cm.

Table 2 is composite shielding properties [28, 34], this table evaluates the effect of combining lead with other materials to enhance shielding while reducing cost and weight [9, 41, 55, 56]. Pb + Fe shows the most significant improvement, with an LAC of  $0.727 \text{ cm}^{-1}$  and HVL of 0.982 cm, combining structural strength with effective attenuation. Pb + Cement and

Pb + Clay combinations show moderate improvements over their base materials, but still fall short of the performance achieved with pure lead or Pb + Fe. Table 3 is the comparative overview this table consolidates data from Tables 1 and 2, providing a unified comparison of pure and composite materials. It confirms that lead remains the benchmark in gamma shielding. The Pb + Fe composite achieves “very good” performance, making it a viable alternative where full lead shielding is impractical. Other composites (Pb + Cement and Pb + Clay) offer incremental gains, which may be useful in applications prioritizing cost or availability over maximum attenuation [57]. Figure 1 presents the linear attenuation coefficient (LAC) comparison of individual materials. This figure likely presents a bar chart comparing the LAC values of individual shielding materials such as Lead ( $1.121\text{ cm}^{-1}$ ), Iron ( $0.463\text{ cm}^{-1}$ ), Concrete ( $0.151\text{ cm}^{-1}$ ), Cement ( $0.139\text{ cm}^{-1}$ ), and Clay ( $0.101\text{ cm}^{-1}$ ). The results clearly indicate that Lead (Pb) provides the highest attenuation capability, making it the most effective shielding material due to its high atomic number and density. Iron offers a practical balance between performance and structural utility.

Materials like cement, concrete [41], and especially clay show lower attenuation values, reflecting their limited effectiveness for high-energy gamma shielding unless used in large thicknesses. Figure 2 displays the half-value Layer (HVL) comparison of individual materials. This chart likely visualizes HVL values, showing the thickness of material needed to reduce gamma intensity by 50%. As expected, Lead has the lowest HVL ( $0.617\text{ cm}$ ), confirming its superior shielding ability. Iron, with an HVL of  $1.496\text{ cm}$ , performs well but requires a thicker barrier. The HVL values increase significantly for concrete ( $4.593\text{ cm}$ ), cement ( $4.965\text{ cm}$ ), and especially clay ( $6.779\text{ cm}$ ), showing that these materials are less efficient and require larger volumes to achieve comparable protection. Figure 3 presents composite material LAC and HVL performance, this figure likely displays the enhanced LAC and reduced HVL values for composite materials: Pb + Fe, Pb + Cement, and Pb + Clay. The Pb + Fe composite achieves a notable improvement ( $\text{LAC} = 0.727\text{ cm}^{-1}$ ,  $\text{HVL} = 0.982\text{ cm}$ ), combining Lead's high attenuation with Iron's structural properties. Pb + Cement and Pb + Clay offers moderate enhancements but still fall short of Pb + Fe. These combinations suggest potential in practical applications where full lead shielding is impractical due to cost or toxicity concerns. Figure 4 is comparative shielding performance (Summary Figure), this figure likely compiles all materials—individual and composite into a single comparative plot of LAC and HVL. It reinforces earlier observations: Lead dominates in attenuation efficiency; composites, particularly Pb + Fe, offer a promising compromise between performance and practicality. Clay remains the least efficient material across all metrics. The figure provides a comprehensive overview, supporting the recommendation for adopting optimized composite shielding in radiation-sensitive environments, especially where weight, cost, or environmental concerns limit pure lead usage.

Lead (Pb) is traditionally regarded as the gold standard in gamma radiation shielding due to its high density ( $11.34\text{ g/cm}^3$ ) and high atomic number ( $Z = 82$ ), it also comes with several significant limitations both in practical applications and environmental contexts. These limitations have increasingly driven interest in alternative and composite shielding materials. Below is a detailed discussion of lead's main drawbacks. While lead remains effective for gamma

shielding, its toxicity, weight, mechanical limitations, and regulatory restrictions make it less suitable for many modern applications. Consequently, research has shifted toward lead-free or composite shielding materials such as heavy concrete, high-Z polymer composites iron-loaded materials and nanostructured or hybrid shielding systems.

**Table 1.** Gamma Shielding Properties shows density, linear attenuation coefficient (LAC), and half-value layer (HVL) for individual materials

Material	Density ( $\text{g/cm}^3$ )	LAC ( $\text{cm}^{-1}$ )	HVL (cm)	Shielding Rank
Lead (Pb)	11.34	1.121	0.617	Excellent
Iron (Fe)	7.87	0.463	1.496	Good
Concrete	2.37	0.151	4.593	Fair
Cement	2.14	0.139	4.965	Moderate
Clay	1.34	0.101	6.779	Poor

**Table 2.** Composite shielding properties highlights the improved performance when combining lead with other materials

Composite	LAC ( $\text{cm}^{-1}$ )	HVL (cm)	Remarks
Pb + Fe	0.727	0.982	Very Good
Pb + Cement	0.15	4.63	Improved
Pb + Clay	0.115	6.066	Slightly Improved

**Table 3.** Comparative shielding performance of building and metallic materials against gamma radiation

Material	Density ( $\text{g/cm}^3$ )	LAC ( $\text{cm}^{-1}$ )	HVL (cm)	Shielding Rank
Lead (Pb)	11.34	1.121	0.617	Excellent
Iron (Fe)	7.87	0.463	1.496	Good
Concrete	2.37	0.151	4.593	Fair
Cement	2.14	0.139	4.965	Moderate
Clay	1.34	0.101	6.779	Poor
Pb + Fe	9.61	0.727	0.982	Very Good
Pb + Cement	6.74	0.150	4.630	Improved
Pb + Clay	6.34	0.115	6.066	Slightly Improved

Iron is ideal where mechanical strength and moderate shielding are needed, concrete and cement are preferred for permanent structures and cost-effective large-scale protection, clay serves well in rural or natural constructions and can be upgraded with additives, research into composite materials (e.g., Pb+Fe, cement with metal oxides) continues to explore how these materials can be enhanced to offer lighter, safer, and affordable alternatives to traditional lead shielding.

Challenges of composite or hybrid shielding materials, material compatibility, homogeneity and fabrication lower overall density complexity in modeling and Simulation moisture and thermal sensitivity regulatory and certification barriers. Composite and hybrid materials hold significant promise in modern radiation shielding, offering a path toward lighter, safer, and more sustainable solutions. However, careful material design, testing, and regulatory validation are essential to overcome technical and practical limitations.

As radiation-based technologies continue to expand across medical, industrial, nuclear, and aerospace sectors, the development of novel shielding materials and designs holds transformative potential for enhancing safety, efficiency, and versatility in radiation protection. Novel shielding materials

and designs are set to revolutionize radiation protection across disciplines. By combining material science, nanotechnology, and advanced manufacturing, future shielding systems will be: More efficient, Safer for users and the environment, Tailored to specific operational contexts. This progress not only enhances radiation safety standards but also enables

broader use of ionizing radiation in fields like precision medicine, clean energy, and aerospace exploration.

Lead clearly outperforms others with the highest LAC and lowest HVL, while composites like Pb + Fe also show significant improvements over basic construction materials like cement and clay as shown in Figure 3.

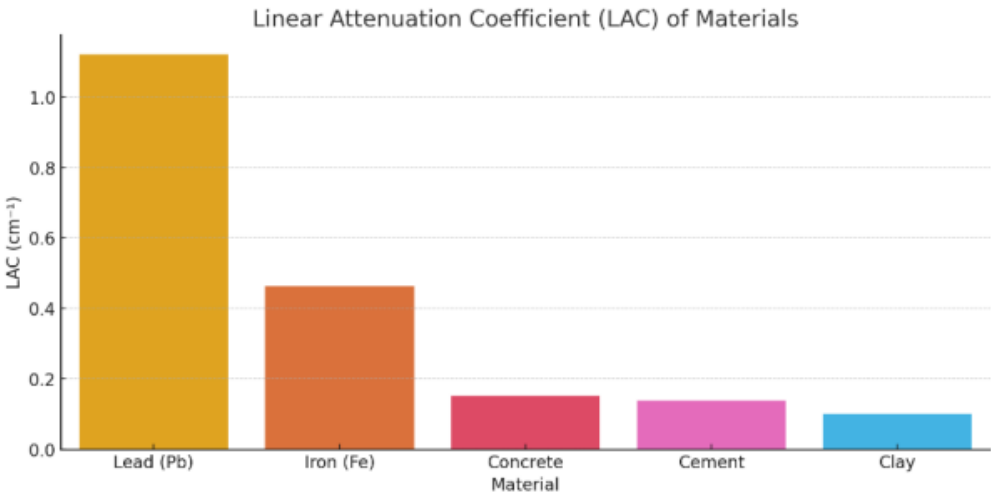


**Figure 1.** The linear attenuation coefficient (LAC) comparison of individual materials

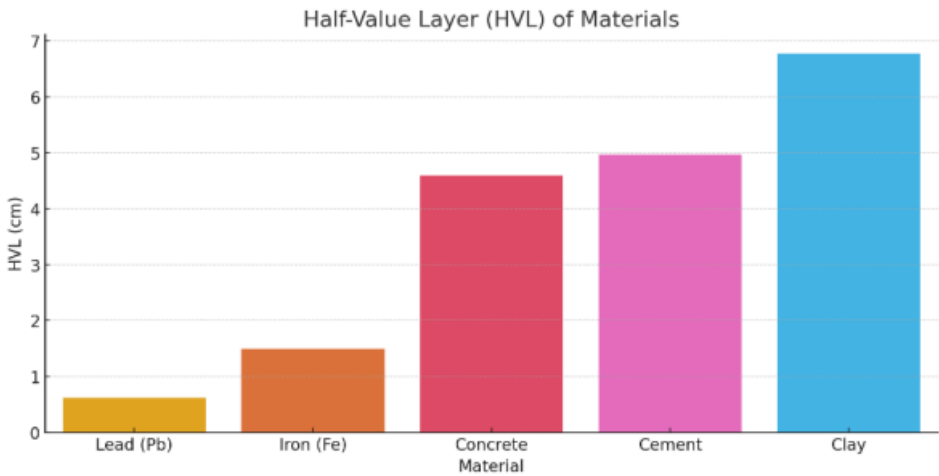


**Figure 2.** Comparison LAC and HVL for each material to visually demonstrate their shielding effectiveness

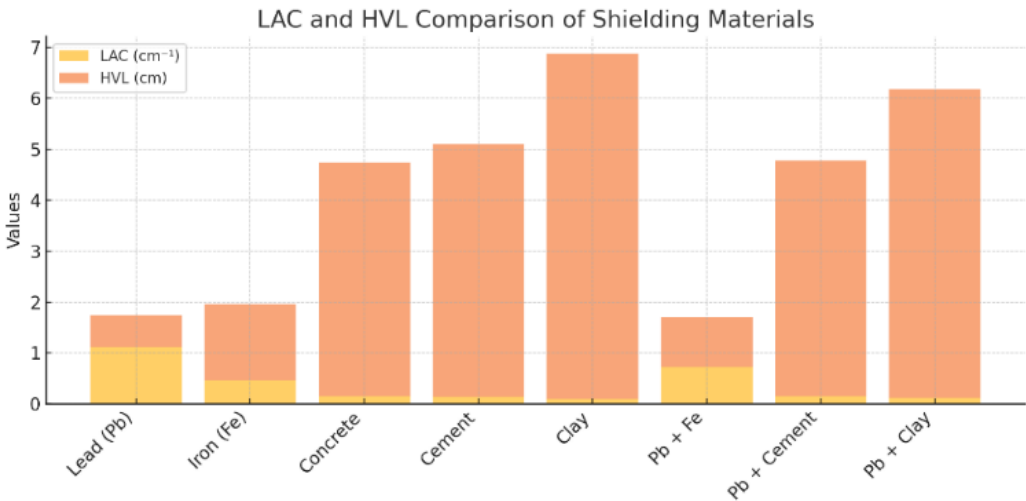


**Figure 3.** Comparison of the linear attenuation coefficient (LAC) and half value layer (HVL) for various shielding materials

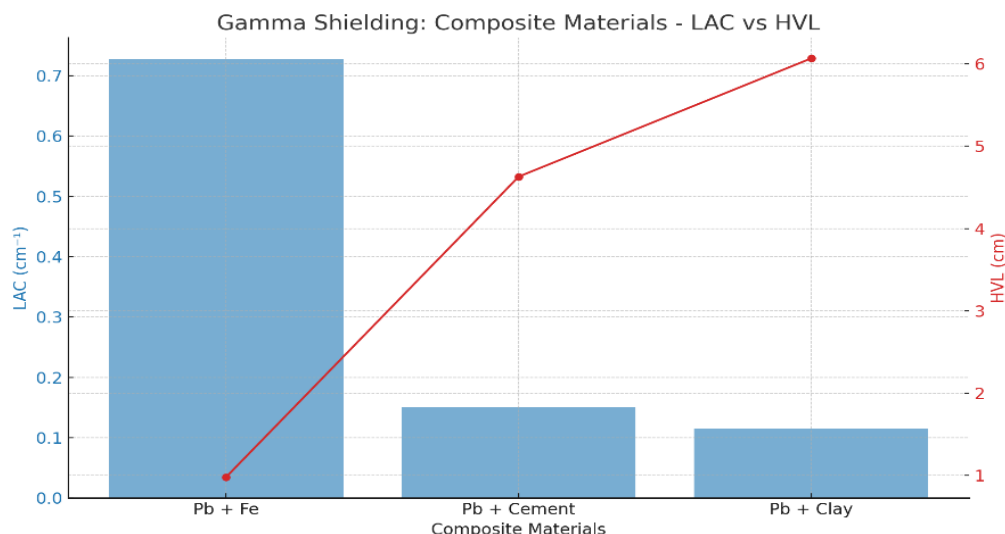


**Figure 4.** Comparison of the gamma shielding performance of different composite materials: Fe also show significant improvements over basic construction materials like cement and clay

#### 4. CONCLUSIONS

This study compares the shielding performance of lead against gamma radiation. Lead is better at shielding because it is dense and has a high atomic number. These properties lead to its excellent linear attenuation coefficient (LAC) and minimal half-value layer (HVL). However, despite these advantages, the practical use of lead is often limited by significant drawbacks. These include high cost, substantial weight, environmental toxicity, and limited availability in certain regions. The exploration of alternative materials is necessary because of these constraints. These materials must be able to offer effective radiation protection without the disadvantages associated with the current materials. It has been demonstrated by the analysis that varying degrees of gamma attenuation are provided by materials like iron, concrete, cement, and clay, but high shielding efficiency may not be achieved by their performance alone for applications requiring it. However, when combined with lead in layered or composite configurations, noticeable improvements in shielding effectiveness can be achieved. Examples include Pb + Fe, Pb + Cement, and Pb + Clay. A promising middle ground is offered by these composites, as the superior attenuation properties of lead are combined with the structural, economic, and handling benefits of lighter and more abundant materials. In the future, research should focus on creating new composite shielding materials that are affordable, lightweight, and eco-friendly, as well as easy to get. Investigations into a variety of materials, including composite structures, recycled industrial by-products, and polymer-metal hybrids, may offer innovative solutions. In addition, advanced modeling and simulation tools should be used to optimize material combinations and geometries for specific radiation environments. The goal is to produce high-performance shielding materials that are scalable for widespread use in medical, industrial, nuclear, and space applications, thereby enhancing both occupational and public radiation safety.

#### ACKNOWLEDGEMENTS

The authors extend their appreciation to the Deanship of

Scientific Research at Northern Border University, Arar, KSA for funding this research work through the project number "NBU-FFR-2025-52-02."

#### REFERENCES

- [1] AlMisned, G., Tekin, H.O., Ene, A., Issa, S.A.M., Kilic, G., Zakaly, H.M.H. (2021). A closer look on nuclear radiation shielding properties of  $\text{Eu}^{3+}$  doped heavy metal oxide glasses: Impact of  $\text{Al}_2\text{O}_3$  / $\text{PbO}$  substitution. *Materials*, 14(18): 5334. <https://doi.org/10.3390/ma14185334>
- [2] Tekin, H.O., Almisned, G., Susoy, G., Zakaly, H.M.H., Issa, S.A.M., Kilic, G., Rammah, Y.S., Lakshminarayana, G., Ene, A. (2022). A detailed investigation on highly dense CuZr bulk metallic glasses for shielding purposes. *Open Chemistry*, 20(1): 69-80. <https://doi.org/10.1515/chem-2022-0127>
- [3] Almisned, G., Zakaly, H.M.H., Issa, S.A.M., Ene, A., Kilic, G., Bawazeer, O., Almatar, A., Shamsi, D., Rabaa, E., Sideig, Z., Tekin, H.O. (2021). Gamma-ray protection properties of bismuth-silicate glasses against some diagnostic nuclear medicine radioisotopes: A comprehensive study. *Materials*, 14(21): 1-11. <https://doi.org/10.3390/ma14216668>
- [4] Tekin, H.O., Almisned, G., Zakaly, H.M.H., Zamil, A., Khouchich, D., Bilal, G., Al-Sammarraie, L., Issa, S.A.M., Al-Buriah, M.S., Ene, A. (2022). Gamma, neutron, and heavy charged ion shielding properties of  $\text{Er}^{3+}$ -doped and  $\text{Sm}^{3+}$ -doped zinc borate glasses. *Open Chemistry*, 20(1): 130-145. <https://doi.org/10.1515/chem-2022-0128>
- [5] Faicdh, I.G. (2005). Shield calculation design for gamma-ray sterilizer plant. *Baghdad Science Journal*, 2(1): 131-134. <https://doi.org/10.21123/bsj.2005.593>
- [6] Al Rawi, K.R.A. (2010). Design and testing a neutrons and Gamma-rays multilayer shield using different groups of cross – sections. *Baghdad Science Journal*, 7(3): 1120-1126. <https://doi.org/10.21123/bsj.2010.7.3.1120-1126>
- [7] Mann, K.S., Mann, S.S. (2021). Py-MLBUF: Development of an online-platform for gamma-ray

- shielding calculations and investigations. *Annals of Nuclear Energy*, 150: 107845. <https://doi.org/10.1016/j.anucene.2020.107845>
- [8] Mann, K.S. (2019). Investigation of gamma-ray shielding by double layered enclosures. *Radiation Physics and Chemistry*, 159: 207-221. <https://doi.org/10.1016/j.radphyschem.2019.03.007>
- [9] Mann, H.S., Brar, G.S., Mann, K.S., Mudahar, G.S. (2016). Experimental investigation of clay fly ash bricks for gamma-ray shielding. *Nuclear Engineering and Technology*, 48(5): 1230-1236. <https://doi.org/10.1016/j.net.2016.04.001>
- [10] İçelli, O., Mann, K.S., Yalçın, Z., Orak, S., Karakaya, V. (2013). Investigation of shielding properties of some boron compounds. *Annals of Nuclear Energy*, 55: 341-350. <https://doi.org/10.1016/j.anucene.2012.12.024>
- [11] Abdullahi, S., Ismail, A.F., Samat, S. (2019). Determination of indoor doses and excess lifetime cancer risks caused by building materials containing natural radionuclides in Malaysia. *Nuclear Engineering and Technology*, 51(1): 325-336. <https://doi.org/10.1016/j.net.2018.09.017>
- [12] Gurau, D. (2024). Reviewing the role of the radiological characterization laboratory in nuclear facility decommissioning. *Acta Physica Polonica A*, 146(2): 165-173. <https://doi.org/10.12693/APhysPolA.146.165>
- [13] Hameed, B.S., Kaddoori, F.F., Fzaa, W.T. (2021). Concentrations and radiation hazard indices of naturally radioactive materials for flour samples in Baghdad markets. *Baghdad Science Journal*, 18(3): 649-654. <https://doi.org/10.21123/BSJ.2021.18.3.0649>
- [14] Abdullah, A.A., Elias, M.M., Shafiq, S.S. (2004). Monitoring of defects concentration in deformed aluminum using doppler broadening technique. *Baghdad Science Journal*, 1: 149-153.
- [15] Elsafi, M., Dib, M.F., Mustafa, H.E., Sayyed, M.I., Khandaker, M.U., Alsubaie, A., Almalki, A.S.A., Abbas, M.I., El-Khatib, A.M. (2021). Enhancement of ceramics based red-clay by bulk and nano metal oxides for photon shielding features. *Materials*, 14(24): 7878. <https://doi.org/10.3390/ma14247878>
- [16] Martin, J.E. (2013). *Atoms, Radiation, and Radiation Protection: Introduction to Radiological Physics and Radiation Dosimetry*. <https://www.ncbi.nlm.nih.gov/books/NBK557499/>.
- [17] Obaid, S.S., Sayyed, M.I., Gaikwad, D.K., Pawar, P.P. (2018). Attenuation coefficients and exposure buildup factor of some rocks for gamma ray shielding applications. *Radiation Physics and Chemistry*, 148: 86-94. <https://doi.org/10.1016/j.radphyschem.2018.02.026>
- [18] Obaid, S.S., Gaikwad, D.K., Pawar, P.P. (2018). Determination of gamma ray shielding parameters of rocks and concrete. *Radiation Physics and Chemistry*, 144: 356-360. <https://doi.org/10.1016/j.radphyschem.2017.09.022>
- [19] Akman, F., Kaçal, M.R., Sayyed, M.I., Karatas, H.A. (2019). Study of gamma radiation attenuation properties of some selected ternary alloys. *Journal of Alloys and Compounds*, 782: 315-322. <https://doi.org/10.1016/j.jallcom.2018.12.221>
- [20] Akman, F., Agar, O., Kaçal, M.R., Sayyed, M.I. (2019). Comparison of experimental and theoretical radiation shielding parameters of several environmentally friendly materials. *Nuclear Science and Techniques*, 30(7): 110. <https://doi.org/10.1007/s41365-019-0631-1>
- [21] Hassan, H.E., Badran, H.M., Aydarous, A., Sharshar, T. (2015). Studying the effect of nano lead compounds additives on the concrete shielding properties for  $\gamma$ -rays. *Nuclear Instruments and Methods in Physics Research, Section B: Beam Interactions with Materials and Atoms*, 360: 81-89. <https://doi.org/10.1016/j.nimb.2015.07.126>
- [22] Liu, C., Benotto, M., Ungar, K., Chen, J. (2022). Environmental monitoring and external exposure to natural radiation in Canada. *Journal of Environmental Radioactivity*, 243: 106811. <https://doi.org/10.1016/j.jenvrad.2022.106811>
- [23] Kerur, B.R., Lagare, M.T. (2009). Mass attenuation coefficient of saccharides for X-rays in the energy range from 8keV to 32keV. *Radiation Measurements*, 44(1): 63-67. <https://doi.org/10.1016/j.radmeas.2008.11.003>
- [24] Kerur, B.R., Rajeshwari, T., Siddanna, R., Kumar, A.S. (2013). Implication and hazard of radiation level in the building materials. *Acta Geophysica*, 61(4): 1046-1056. <https://doi.org/10.2478/s11600-013-0109-1>
- [25] Madbouly, A.M., El- Sawy, A.A. (2018). Calculation of gamma and neutron parameters for some concrete materials as radiation shields for nuclear facilities. *International Journal of Emerging Trends in Engineering and Development*, 3(8): 7-17. <https://doi.org/10.26808/rs.ed.i8v4.02>
- [26] Sallam, O.I., Madbouly, A.M., Elalaily, N.A. (2020). Physical properties and radiation shielding parameters of bismuth borate glasses doped transition metals. *Journal of Alloys and Compounds*, 843: 156056. <https://doi.org/10.1016/j.jallcom.2020.156056>
- [27] Sallam, O.I., Rammah, Y.S., Nabil, I.M., El-Seidy, A.M.A. (2024). Enhanced optical and structural traits of irradiated lead borate glasses via  $Ce^{3+}$  and  $Dy^{3+}$  ions with studying Radiation shielding performance. *Scientific Reports*, 14(1): 24478. <https://doi.org/10.1038/s41598-024-73892-w>
- [28] Al-Hadeethi, Y., Sayyed, M.I. (2020). Using Phy-X/PSD to investigate gamma photons in  $SeO_2$ - $Ag_2O$ - $TeO_2$  glass systems for shielding applications. *Ceramics International*, 46(8): 12416-12421. <https://doi.org/10.1016/J.CERAMINT.2020.02.003>
- [29] Al-hadeethi, Y., Sayyed, M.I., Agar, O. (2020). Ionizing photons attenuation characterization of quaternary tellurite-zinc-niobium-gadolinium glasses using Phy-X / PSD software. *Journal of Non-Crystalline Solids*, 538: 120044. <https://doi.org/10.1016/j.jnoncrysol.2020.120044>
- [30] Darwesh, R., Sayyed, M.I., Al-Hadeethi, Y., Alotaibi, J.S. (2025). Synthesis and characterization of  $TeO_2$ - $B_2O_3$ - $CaO$ - $ZnO$  glass systems for improved radiation shielding performance. *Journal of Radiation Research and Applied Sciences*, 18(1): 101259. <https://doi.org/10.1016/j.jrras.2024.101259>
- [31] Bantan, R.A.R., Sayyed, M.I., Mahmoud, K.A., Al-Hadeethi, Y. (2020). Application of experimental measurements, Monte Carlo simulation and theoretical calculation to estimate the gamma ray shielding capacity of various natural rocks. *Progress in Nuclear Energy*, 126: 103405. <https://doi.org/10.1016/j.pnucene.2020.103405>
- [32] Rammah, Y.S. (2019). Evaluation of radiation shielding ability of boro-tellurite glasses:  $TeO_2$ - $B_2O_3$ - $SrCl_2$ - $LiF$ - $Bi_2O_3$ . *Applied Physics A: Materials Science and*



- Processing, 125(12): 857.  
<https://doi.org/10.1007/s00339-019-3154-z>
- [33] Al-Buriah, M.S., Rammah, Y.S. (2019). Electronic polarizability, dielectric, and gamma-ray shielding properties of some tellurite-based glasses. *Applied Physics A: Materials Science and Processing*, 125(10): 678. <https://doi.org/10.1007/s00339-019-2976-z>
- [34] Zakaly, H.M.H., Rammah, Y.S., Tekin, H.O., Ene, A., Badawi, A., Issa, S.A.M. (2022). Nuclear shielding performances of borate/sodium/potassium glasses doped with  $\text{Sm}^{3+}$  ions. *Journal of Materials Research and Technology*, 18: 1424-1435. <https://doi.org/10.1016/j.jmrt.2022.03.030>
- [35] Al-Omari, S., Afaneh, F., Alsaif, N.A.M., Al-Ghamdi, H., Rammah, Y.S., Khattari, Z.Y. (2024). Optimization radiation shielding properties of aluminum-based spinel minerals through the crystal tetrahedral and octahedral voids and their ions composition. *Radiation Physics and Chemistry*, 217: 1-10. <https://doi.org/10.1016/j.radphyschem.2024.111527>
- [36] Alsaif, N.A.M., Khattari, Z.Y., Zakaly, H.M.H., Rammah, Y.S., Ene, A., Al-Buriah, M.S. (2023). Mechanic-elastic properties and radiation attenuation efficiency of  $\text{TeO}_2/\text{WO}_3/\text{K}_2\text{O}$  composite glass systems for nuclear and medical application. *Heliyon*, 9(8): e18912. <https://doi.org/10.1016/j.heliyon.2023.e18912>
- [37] Cook, A., Meggitt, G.C. (1979). Radiological protection. *Energy Dig*, 8(2): 16-19. <https://doi.org/10.4324/9780203020746-18>
- [38] Protection, R. (2003). Radiation protection practice/evaluation. *Radiation Protection and Dosimetry*, 244-308. [https://doi.org/10.1007/978-0-387-49983-3\\_11](https://doi.org/10.1007/978-0-387-49983-3_11)
- [39] Tyagi, G., Singhal, A., Routroy, S., Bhunia, D., Lahoti, M. (2021). Radiation Shielding Concrete with alternate constituents: An approach to address multiple hazards. *Journal of Hazardous Materials*, 404: 124201. <https://doi.org/10.1016/j.jhazmat.2020.124201>
- [40] Xu, H., Liu, D., Sun, W.Q., Wu, R.J., Liao, W., Li, X.L., Hu, G., Hu, H.S. (2022). Study on the design, preparation, and performance evaluation of heat-resistant interlayer-polyimide-resin-based neutron-shielding materials. *Materials*, 15(9): 2978. <https://doi.org/10.3390/ma15092978>
- [41] Mohamed E.M. Eisa, M.D. M. Ali, M.J.A. (2023). Study of Gamma-ray shielding of two different heavy metals and their combination for Cs-137 and Co-60 Sources. *Engineering, Technology & Applied Science Research*, 13(1). <https://www.etasr.com/index.php/ETASR/article/view/5513>
- [42] Kato, M., Ishii, J., Tanaka, H., Sugiyama, M., Kurosawa, T. (2024). Portable gamma irradiation system with  $^{57}\text{Co}$ ,  $^{133}\text{Ba}$ ,  $^{137}\text{Cs}$ , and  $^{60}\text{Co}$  for on-site calibration of environmental radiation monitoring devices. *Journal of Radiation Protection and Research*, 49(4): 166-173. <https://doi.org/10.14407/jrpr.2024.00066>
- [43] AL-Dhuhaibat, M.J.R. (2015). Study of the shielding properties for some composite materials manufactured from polymer epoxy supported by cement, aluminum, iron and lead against gamma rays of the cobalt radioactive source (Co-60). *International Journal of Application or Innovation in Engineering & Management (I JAI EM)*, 4(6): 90-98.
- [44] Gili, M.B.Z., Hila, F.C. (2021). Investigation of gamma-ray shielding features of several clay materials using the EPICS2017 library. *Philippine Journal of Science*, 150(5): 1017-1026.
- [45] Gili, M.B.Z., Hila, F.C. (2021). Characterization and radiation shielding properties of Philippine natural bentonite and zeolite. *Philippine Journal of Science*, 150(6A): 1475-1488.
- [46] Sayyed, M.I. (2017). Half value layer, mean free path and exposure buildup factor for tellurite glasses with different oxide compositions. *Journal of Alloys and Compounds*, 695: 3191-3197. <https://doi.org/10.1016/j.jallcom.2016.11.318>
- [47] Sayyed, M.I. (2016). Investigation of shielding parameters for smart polymers. *Chinese Journal of Physics*, 54(3): 408-415. <https://doi.org/10.1016/j.cjph.2016.05.002>
- [48] Elsafi, M., Koraim, Y., Almurayshid, M., Almasoud, F.I., Sayyed, M.I., Saleh, I.H. (2021). Investigation of photon radiation attenuation capability of different clay materials. *Materials*, 14(21): 6702. <https://doi.org/10.3390/ma14216702>
- [49] Isinkaye, M.O., Jibiri, N.N., Bamidele, S.I., Najam, L.A. (2018). Evaluation of radiological hazards due to natural radioactivity in bituminous soils from tar-sand belt of southwest Nigeria using HpGe-detector. *International Journal of Radiation Research*, 16(3): 351-362. <https://doi.org/10.18869/acadpub.ijrr.16.3.351>
- [50] Lacomme, E., Sayyed, M.I., Sidek, H.A.A., Matori, K.A., Zaid, M.H.M. (2021). Effect of bismuth and lithium substitution on radiation shielding properties of zinc borate glass system using Phy-X/PSD simulation. *Results in Physics*, 20: 103768. <https://doi.org/10.1016/j.rinp.2020.103768>
- [51] Gerward, L., Guilbert, N., Jensen, K.B., Levring, H. (2004). WinXCom - A program for calculating X-ray attenuation coefficients. *Radiation Physics and Chemistry*, 71(3-4): 653-654. <https://doi.org/10.1016/j.radphyschem.2004.04.040>
- [52] Singh, R., Singh, S., Singh, G., Thind, K.S. (2017). Gamma radiation shielding properties of steel and iron slags. *New Journal of Glass and Ceramics*, 7(1): 1-11. <https://doi.org/10.4236/njgc.2017.71001>
- [53] Singh, K.J., Singh, N., Kaundal, R.S., Singh, K. (2008). Gamma-ray shielding and structural properties of  $\text{PbO}-\text{SiO}_2$  glasses. *Nuclear Instruments and Methods in Physics Research Section B: Beam Interactions with Materials and Atoms*, 266(6): 944-948. <https://doi.org/10.1016/j.nimb.2008.02.004>
- [54] D'Souza, A.N., Madivala, S.G., Saraswathi, A.V., Sayyed, M.I., Rashad, M., Kamath, S.D. (2025). Impact of Co-doping  $\text{Eu}^{3+}$  and  $\text{Gd}^{3+}$  in HMO-based glasses for structural and optical properties and radiation shielding enhancement. *Luminescence*, 40(1): e70045. <https://doi.org/10.1002/bio.70045>
- [55] Vu, H.Q., Tran, V.H., Nguyen, P.T., Le, N.T.H., Le, M.T. (2020). Radiation shielding properties prediction of barite used as small aggregate in Mortar. *Engineering, Technology & Applied Science Research*, 10(6): 6469-6475. <https://doi.org/10.48084/etasr.3880>
- [56] Jarupreedeephad, K., Chaiphaksa, W., Wiwatkanjana, P., Kaewkhao, J. (2019). Theoretical calculation of mass attenuation coefficient and radiation shielding parameters of  $\text{WO}_3\text{-TeO}_3$  glasses. *Journal of Physics: Conference Series*, 1259(1): 012010.



<https://doi.org/10.1088/1742-6596/1259/1/012010>  
[57] Al-Buriahi, M.S., Eke, C., Alomairy, S., Mutuwong, C.,  
Sfina, N. (2021). Micro-hardness and gamma-ray  
attenuation properties of lead iron phosphate glasses.

Journal of Materials Science: Materials in Electronics,  
32(10): 13906-13916. <https://doi.org/10.1007/s10854-021-05966-8>